



DRAG REDUCTION INDUCED BY FLEXIBLE AND RIGID MOLECULES IN A TURBULENT FLOW INTO A ROTATING CYLINDRICAL DOUBLE GAP DEVICE: COMPARISON BETWEEN POLY(ETHYLENE OXIDE), POLYACRYLAMIDE, AND XANTHAN GUM

Anselmo Soeiro Pereira

Rafhael Milanezi de Andrade

Department of Mechanical Engineering, Universidade Federal do Espírito Santo, Avenida Fernando Ferrari, 514, Goiabeiras, 29075-910, ES, Brazil

anselmospereira@gmail.com and rafhaelmilanezi@gmail.com

Edson José Soares

Department of Mechanical Engineering, Universidade Federal do Espírito Santo, Avenida Fernando Ferrari, 514, Goiabeiras, 29075-910, ES, Brazil

edson@ct.ufes.br

Abstract. *Polymer-induced drag reducing flow has been investigated for over 60 years. However, the phenomenon is not completely understood. Some important issues are related to the development of turbulent structures and to the breaking of the polymer molecules. These two phenomena impose a transient behavior on the polymer efficiency and the drag reduction, DR, can be clearly divided into three periods of time: the very beginning period, the polymer degradation and the asymptotic drag reduction. In the present paper, we study the drag reduction development from the very beginning of a turbulent flow into a rotating cylindrical double gap device. The DR is induced by three different polymers: Poly(ethylene oxide) (PEO), Polyacrylamide (PAM) and Xanthan Gum (XG). The first two are known as flexible molecules while the last one is considered rigid. The goal here is to compare the effect of the different polymers on the DR over time, paying particular attention to the difference between the rigid and the flexible molecules. The tests are conducted for a range of Reynolds numbers, concentrations and temperatures, from the very start to the time when the drag reduction achieves its final level of efficiency.*

Keywords: *Drag reduction, polymer degradation, development time, flexible and rigid molecules*

1. INTRODUCTION

Polymeric drag reducers have been successfully used in a number of applications for more than 60 years (see Fabula (1971), Burger and Chorn (1980), Greene *et al.* (1980) and Sellin *et al.* (1982)). Over the years, researchers have been successful in analysing this phenomenon and many remarkable papers with practical interest can be found (see Virk *et al.* (1967), Virk *et al.* (1970), Virk (1975a), Virk (1975b) and Moussa and Tiu (1994)). Up to now, there has been no generally accepted theory for the mechanism of drag reduction, despite the fact that many researchers have contributed with some very significant papers (see Lumley (1969), Tabor and de Gennes (1986), Dubief *et al.* (2004) and Benzi (2010)). White and Mungal (2008) is a good review of some recent progress in understanding the fundamentals of polymer drag reduction.

The drag reduction phenomenon is very dependent on the kind of drag reducer used. Commonly, fibrous particles, surfactants and polymers are used. These last are very far more efficient and have been widely analyzed over the years. Concerning their mechanical resistance, polymers can be divided into flexible and rigid molecules. The former are generally of high molecular weight with a linear chain, among which Poly(ethylene oxide), Polyacrylamide and Polyisobutylene are examples which have been extensively tested over the years (see Virk *et al.* (1967), Paterson and Abernathy (1970), Kenis (1971), Peyser and Little (1971), Virk (1975b), Berman (1978), Sellin *et al.* (1982), Deshmukh and Singh (1986), Rho *et al.* (1996), Choi and Jhon (1996), Kim *et al.* (1997), Kalashnikov (1998), Kalashnikov (2002), Choi *et al.* (2001) and Bizoto and Sabadini (2008)). An huge disadvantage, which is a great obstacle to the practical use of flexible polymers is their mechanical degradation. A possibility that deserves our attention is the use of polysaccharides such as Hydroxypropylguar, Gar Gum and Xanthan Gum (see Kim *et al.* (1985); Deshmukh and Singh (1986) and S. Chakrabarti and Brunn (1991b)). Such molecules are rigid and much less susceptible to mechanical scission. The main problem in this case is the biological degradation, though it is much less accelerated when compared to the mechanical scission.

Among the different rigid polymers known in the literature, Xanthan Gum seems to be of particular practical interest in food, pharmaceuticals, cosmetics, and the oil industry, in which it is widely used as a drag reducer in drilling well operations. From the molecular point of view, XG possesses a linear main chain of (1-4)- β -D glucose, similar to cellulose, with a trisaccharide side chain on every second D-glucose (see Bewersdorff and Singh (1988) for details). In fact, such a complex structure is responsible for its rigidity and stability. Its structure is highly dependent on the temperature and

salinity. At moderate temperatures and low ionic forces, XG presents a stable organized helical conformation resulting in a rigid molecular structure, as reported by Morris (1977) and Norton *et al.* (1984). Such an organized structure can be modified by increasing temperature or salinity. In such conditions, the ionic forces are altered and the helical configuration changes to a recoiled one. In this new configuration, the Xanthan Gum's capability to reduce drag drops dramatically. In fact, temperature plays a complex role in the structural configuration of XG. Below a certain value of T , known as the *transition-midpoint temperature*, an increase in T causes an increase in the mean molecule length, keeping the helical structure stable as suggested by Sohn *et al.* (2001). The salinity also plays a very important role in the structural configuration of XG. For more details of the mechanism and dynamics of XG's structure, see Morris (1977), Norton *et al.* (1984), and Muller *et al.* (1986).

As with flexible polymers, the drag reduction obtained with the use of Xanthan Gum is an increasing function of its concentration and molecular weight (see Bewersdorff and Singh (1988), Bewersdorff and Berman (1988) and Sohn *et al.* (2001)). Also similar to other polymers, the level of DR achieves an asymptotic value with increasing c and M_v . However, the drag reduction mechanism for rigid polymers seems to be considerably different. Such a difference can be easily noticed observing the Fanning friction factor in Prandtl-Von Kármán coordinates, for example. After the onset, the curves for XG are parallel to the Newtonian one, which suggests a weak dependence on the Reynolds number, as reported by many authors who investigated rigid polymers (Virk (1975a), Bewersdorff and Singh (1988), Bewersdorff and Berman (1988), Sohn *et al.* (2001), and Jaafar *et al.* (2009)). Such an effect is known as *retro-onset* and was discussed by Virk (1975a). *Retro-onset* is generally associated with rigid molecules. According to Virk *et al.* (1997), drag reduction can be divided into two very distinct mechanisms: Type A and Type B. The former is associated with polymers that stay recoiled at rest. Such materials need a certain level of turbulence to stretch and start to reduce drag. In contrast, the second mechanism is related to polymers that stay extended at rest. Consequently, the onset of the drag reduction is expected to occur early when the Type B mechanism is dominant. As suggested by Gasljevic *et al.* (2001), in the case of Type B mechanism of drag reduction, polymer molecules may be fully stretched after the retro-onset, and, consequently, a further increase in the level of turbulence could not result in a substantial change of molecular conformation. The mechanism of drag reduction for Xanthan Gum solutions is clearly of Type B.

A huge obstacle to attempts to obtain an accepted theory of the phenomenon of drag reduction is the mechanical molecular degradation. This issue involves a strong interdisciplinary connection between chemistry and fluid mechanics. This issue has received deserved attention over the years and many aspects of the problem have been studied, such as the effect of concentration, molecular weight, Reynolds number and temperature on the efficiency of drag the reduction (see Paterson and Abernathy (1970), Nakano and Minoura (1975), Yu *et al.* (1979), Tabata *et al.* (1986), Moussa and Tiu (1994), Rho *et al.* (1996) and Pereira and Soares (2012)). Using an experimental turbulent pipe flow apparatus, Vanapalli *et al.* (2005) performed some careful analyses to show that DR decreases as a consequence of polymer degradation but reaches a steady state after a certain number of passes through the pipe flow apparatus. In other words, the molecular scission stops after a long enough time. This tendency is supported by many other results, such as those reported by Nakken *et al.* (2001), Choi *et al.* (2001), Kalashnikov (2002) and Pereira and Soares (2012).

The dependence of drag reduction on time is not exclusively related to molecular degradation. As reported by Dimitropoulos *et al.* (2005), the turbulent structures take some time to rearrange following a polymer deformation and the DR does not achieve its ultimate level instantaneously. In fact, DR is a complicated function of time. Fig. 3 shows schematically the development of a polymer induced near-wall drag reduction, defined as $DR = 1 - f_p/f_0$, where f_p is the friction factor of the polymeric solution and f_0 that of the solvent. This kind of figure can be constructed by monitoring the drag reduction along a pipe or channel after the polymer injection or by using any rotating apparatus. The last strategy is evidently easier. As sketched in Fig. 3, the available results concerning flexible polymers suggest that at the very start of the test, the DR decreases from DR_0 to DR_{min} before achieving its top level of efficiency at DR_{max} . Since polymers extract energy from the vortices and release energy to the mean flow in a coil-stretch cycle, we presume that the maximum drag reduction occurs when a sufficient number of the molecules are in this coil-stretch cycle (Dubief *et al.* (2004)) and a state of equilibrium with the turbulent structures has been achieved. We will refer to the time to achieve DR_{max} as the *developing time*, denoted t_d . The increasing friction factor at the beginning of the process is related to an instantaneous increment of the local extensional viscosity after a high polymer stretching. Following t_d , we observe a constant value of DR for a period of time, which is denoted by t_r , the *resistance time*. Finally, after this period, DR begins to fall, reaching a minimum level after a long enough time, when the degradation process has reached its steady state and DR assumes an asymptotic value, DR_{asy} . The time to reach DR_{asy} , t_a , is relatively large compared with the stretching time of a single molecule, because the molecules are stretched and degraded step-by-step (see Elbing *et al.* (2011)). Thus, we could presume that during t_r the increasing number of molecules in the coil-stretch cycle is balanced by the molecular degradation, and the ultimate level of drag reduction is sustained. Following that, with a continuous degradation, the turbulent structures depart from their equilibrium and start to increase until achieving the final steady state in which the level of drag reduction assumes a constant value, DR_{asy} . This theory seems to be quite reasonable for flexible polymers but does not explain the behavior of $DR(t)$ for rigid polymers. The coil-stretch process, for example, probably does not play an important role in this kind of material, once the rigid molecules stay almost well-extended at rest.

There have been a number of papers treating DR as a function of time. Recently, Pereira and Soares (2012) showed a great number of data in an attempt to understand the effect of the temperature, Reynolds number, concentration, and molecular weight on t_d , t_r , and t_a , but most of the data is related to PEO solutions. In the present paper, the experiments were conducted in an attempt to provide a direct comparison between PEO, PAM, and XG. The last polymer is a rigid molecule and the results related to it is particularly interesting and it is the main goal of this research.

2. EXPERIMENTAL APPARATUS AND PROCEDURE

In the present work we decided to use a cylindrical double-gap geometry as that used by Nakken *et al.* (2001). A scheme of the apparatus is shown in Fig. 1. Because its large contact area, we can obtain a quite good accuracy with this kind of apparatus and measurements can be obtained in a very small values of Reynolds number. The tests were carried out using a commercial rheometer model HAAKE MARS II manufactured by Thermo Scientific, Germany. The sample is located between the two rigidly interconnected coaxial and stationary surfaces with axial symmetry. The rotor, a coaxial thin-walled tube, is located between these two fixed cylindrical surfaces and can rotate over the sample holder axis of rotation symmetry with a given angular velocity. The radii $R_1 = 17.75$ mm, $R_2 = 18.00$ mm, $R_3 = 21.40$ mm and $R_4 = 21.70$ mm and the rotor height $L = 55.00$ mm, shown on Fig. 1, are the important scales of our test section. The sample volume is 6.3 ml.

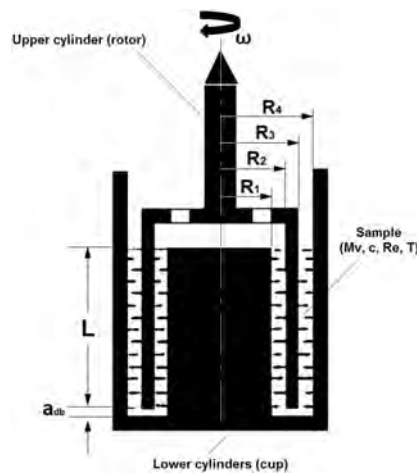


Figure 1. Schematic illustration of the axial symmetric double gap utilized in the present paper.

For a given angular velocity (ω), the mean shear rate ($\dot{\gamma}$) is determined by Eq. (1) as a function of n , the rotor speed of rotation, and $K = \frac{2R_4^2}{R_4^2 - R_3^2} = \frac{2R_2^2}{R_2^2 - R_1^2}$, a geometrical factor.

$$\dot{\gamma} = K\omega = K \frac{2\pi}{60} n. \quad (1)$$

The measured torque on the rotor is related to nominal shear stress, τ , by Eq. (2).

$$T = \frac{4\tau\pi L (\delta^2 R_3^2 + R_2^2)}{1 + \delta^2} \quad (2)$$

Where $\delta = R_4/R_3 = R_2/R_1$ is an aspect ratio. Thus, we can calculate the Fanning friction factor based on the mean radius $\bar{R} = \frac{R_2 + R_3}{2}$ as follow.

$$f = \frac{2\tau}{\rho u^2} = \frac{2\tau}{\rho (\omega \bar{R})^2}. \quad (3)$$

The Reynolds number is defined by Eq. (4):

$$Re = \frac{\rho \bar{h} u}{\eta} = \frac{\rho (\bar{h}) (\omega \bar{R})}{\eta}, \quad (4)$$

where η is the solution's viscosity, $\omega \bar{R}$ is a characteristic velocity and \bar{h} is the average gap given by $((R_2 - R_1) + (R_4 - R_3))/2$.

In order to distinguish the distinct flows in the double-gap geometry, for a range of analyzed Reynolds numbers, we used the Taylor number given by Eq. (5)

$$Ta = \frac{\bar{R} \bar{h}^3 \omega^2}{\nu^2}, \quad (5)$$

where ν is the cinematic viscosity.

We tested solutions of Poly(ethylene oxide), Polyacrylamide, and Xanthan Gum. The molecular weight of the first and second materials is $M_v = 5.0 \times 10^6$ g/mol, whereas that of the last one is $M_v = 2.0 \times 10^6$ g/mol. All our chemical supplies were provided by Sigma-Aldrich. We obtained the molecular weight by calculating the intrinsic viscosity using the Huggins equation (for details see Flory (1971)) and our measurements were very close to the values quoted by Sigma-Aldrich. The measured intrinsic viscosity, $[\eta]$, was also used to estimate the overlap concentration for PEO and PAM by means of the relation $c^*[\eta] = 1$. For the PEO solutions, the calculated value was $c^* = 3125$. For the PAM, the overlap concentration was around $c^* = 100$ ppm. This procedure was not used for the XG solutions, as it is highly shear-thinning. An attempt to obtain the overlap concentration of this polymer was conducted by measuring its zero-shear viscosity at different concentrations. There is a value of concentration for which the variation of η_0 is considerably increased, and we suppose that the overlap concentration, c^* , is below such a value. We conducted here the same procedure used by Jaafar *et al.* (2009). By means of this technique, we estimated the overlap concentration of the Xanthan Gum to be $c^* = 940$ ppm. In fact, this technique is not very precise and c^* could be smaller. By means of the same technique Wyatt *et al.* (2011) found c^* around 70 ppm using a Xanthan Gum with the same molecular weight used by this work. The maximum polymer concentration used in this work was 100 ppm which suggests we are working with diluted solutions. Using deionized water as a solvent, the polymer powders were gently deposited on the solvent surfaces. Each test was carried out after 24 hours, time for complete natural diffusion. This procedure was adopted to avoid any polymer degradation before the beginning of the test.

The solution viscosity was measured with the HAAKE MARS II for a range of rotations in which the flow was viscometric. The values measured were compared with that obtained from a capillary viscometer and quite a good agreement was observed. For concentrations smaller than 100 ppm, for both PEO and PAM, no significant shear-thinning behavior was noticed. Such behaviour was only observed for very high concentrations, larger than 1000 ppm. Differently, the Xanthan Gum viscosity has a significant shear thinning behaviour, even for very small concentrations. The shear-thinning behaviour of PEO, PAM (at high concentrations) and XG is quite good fitted by a Carreau-Yasuda like equation.

The maximum rotational speed of the rotor used was $n = 3000$ rpm (revolution per minute). The flow field becomes unstable in Ta , Eq.(5), close to 1700. This value of Ta is achieved when n is close to 500 rpm. This corresponds to $Re = \frac{\rho \bar{h} u}{\eta} \geq 350$. Drag reduction is only observed for values of Ta beyond this critical value. In the main tests, the rotational speed was kept constant to display the drag reduction as a function of time which was extended over 7000 seconds and around 5400 shear stress values were measured.

3. RESULTS AND DISCUSSION

The tests were conducted in attempt to highlight some quantitative and qualitative differences between two types of drag reducers: flexible (PAM and PEO) and rigid (XG) polymers. The results are displayed considering variations in the Reynolds number, concentration, and temperature. We present our results in three parts. In subsection 3.1 we show the Fanning friction factor in Prandtl-von Kármán coordinates for a range of concentrations of each polymer. Subsection 3.2 presents $DR(t)$ over time from the very beginning of the test until reaching its asymptotic value after a long enough time. Finally, in subsection 3.3 we present the time dependent relative drag reduction, $DR'(t)$, where the loss of efficiency, eventually caused by the degradation mechanism, is more clearly discussed.

3.1 FANNING FRICTION FACTOR IN PRANDTL-VON KÁRMÁN COORDINATES

Fig. 2 shows the Fanning friction factor in the Prandtl-von Kármán coordinates for a range of concentrations ($1 \text{ ppm} \leq c \leq 50 \text{ ppm}$) of PEO, PAM, and XG with the temperature fixed at 25°C . The rotation was gradually increased from 0 to 3000 rpm over 5 minutes. As widely reported by a number of researchers, the friction factor falls and the onset of drag reduction occurs at smaller values of Reynolds numbers with increasing concentration. This is clearly observed for the flexible polymers (PEO and PAM) and also for the rigid one (XG), Fig. 2A, B and C. It is also clear that the values of the coefficient ($1/\sqrt{f}$) are more pronounced in the PEO solutions. The smallest values of this parameter are observed in the XG solutions. However, what is worth noting here is the fact that the phenomenon for XG solutions seems to be considerably different. For PEO and PAM solutions, it is clearly observed that the curves at distinct concentrations are moving away from each other with increasing Reynolds number. In contrast, the lines displayed for each concentration of XG, after the onset, seem to be parallel. It is also noticeable that the onset of drag reduction occurs at a much smaller Reynolds number in XG solutions. This is easily perceived for $c = 50$ ppm. This observation suggests that the Reynolds number plays a weak role in Xanthan Gum solutions. Results reported by Bewersdorff and Singh (1988) and Bewersdorff and Berman (1988), using Xanthan Gum, and more recently by Jaafar *et al.* (2009) using Scleroglucan (another well-known rigid-chain polymer), also indicate such an effect of the Reynolds number on the friction factor. The reason for these observations is related to the fact that XG is a rigid polymer and is already extended on its equilibrium state at rest. Hence, our observation is in agreement with the idea of a Type B mechanism of drag reduction reported by Virk *et al.* (1997).

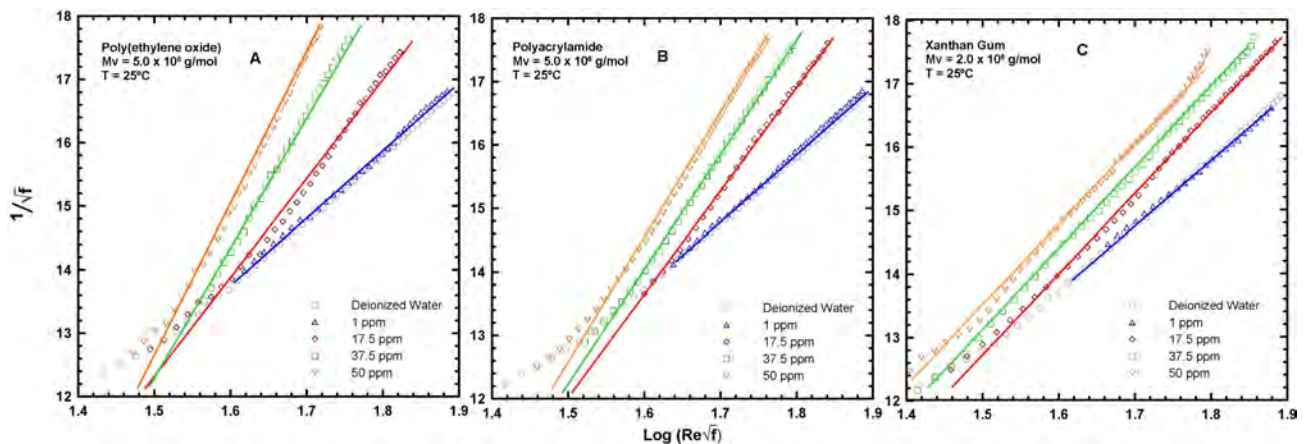


Figure 2. Effects of concentration on Fanning friction factor, f , as a function of Reynolds number, Re . The rotation was gradually increased from 0 to 3000 rpm. The measurements were carried out for PEO, PAM and XG, respectively, A, B and C, at different concentrations, and with the temperature fixed at 25°C. The molecular weight for PEO and PAM was maintained at 5.0×10^6 g/mol whereas there was used a XG with $M_v = 2.0 \times 10^6$ g/mol.

3.2 DRAG REDUCTION DECAY

In this subsection, we display the drag reduction over time to take into account the phenomenon from the very start of the test until the asymptotic value of DR is achieved. The tests were carried out for each polymer at a range of Reynolds numbers, concentrations and temperatures. The dependence of the drag reduction on time can be, at least, divided into three distinct periods. A sketch of $DR(t)$ is shown in Fig. 3. From the very beginning of the test, the DR increases before reaching its maximum efficiency. DR_{max} is not achieved instantaneously because a period of time, *the developing time* t_d , is required for the turbulent structures to arrange after the high degree of polymer deformation at the very start of the test. Such a mechanism was for the first time numerically computed by Dimitropoulos *et al.* (2005) and, as far as we know, experimentally observed by Pereira and Soares (2012). The maximum level of efficiency is sustained for a while, *the resistance time* t_r . Supposedly, when the degradation becomes important, DR starts to decrease until achieving its asymptotic value, a time during which the polymer scission stops and the molecular weight distribution reaches a steady state. A discussion concerning the effect of the Reynolds number, concentration, molecular weight, and temperature on the developing time and the resistance time was reported by Pereira and Soares (2012). The author's analysis considers turbulent flows of PEO and PAM solutions. The explanation for the complex behaviour of $DR(t)$ is related to the delay of the rearrangements of the turbulent structures after the polymer stretching and the mechanical degradation process. Here our main interest is to highlight the main difference between the molecules PEO, PAM, and XG from such a point of view. As mentioned previously, the first and the second are flexible molecules whereas the last is considered a rigid one.

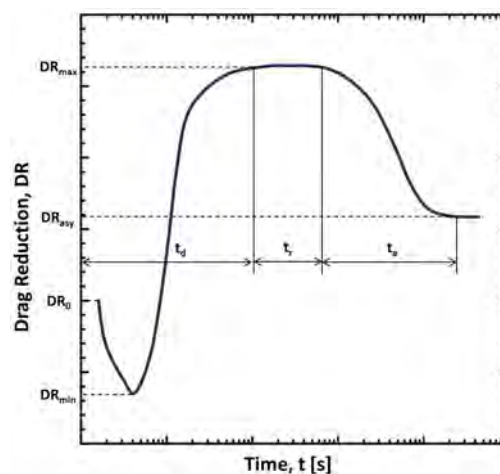
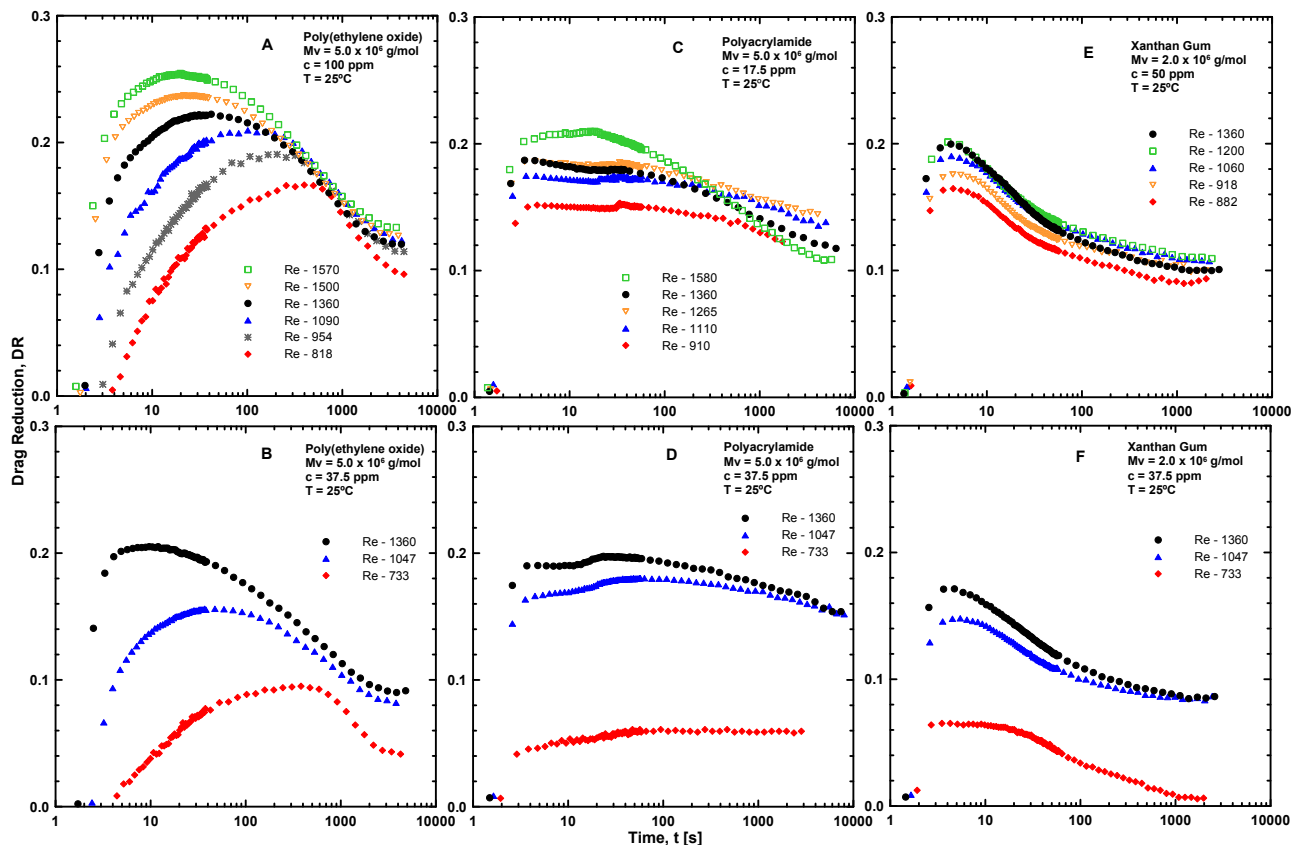


Figure 3. Sketch of the evolution over time of the polymer-induced drag reduction.

Fig. 4 displays DR against time for each polymer (PEO, PAM and XG) for a range of Reynolds numbers at two different concentrations. The temperature was maintained at 25°C. From the top to the bottom, the results are displayed, respectively, for PEO, PAM and XG. We can observe, comparing the figures A and B that the Reynolds number plays a

more important role for the less concentrated solution of PEO. We can clearly see that the curves for the less concentrated solutions are more separated from each other. This is expected considering that the drag reduction by polymers is bounded by a maximum drag reduction asymptote (MDR) and 100 ppm of PEO is very close to the MDR asymptote. Thus, an increase of the Reynolds number value at the less concentrated solution could provide a more significant change of the DR . Moreover, the developing time, t_d , seems to be delayed when the concentration is increased. Such an effect is apparent for PEO solutions, as could be observed comparing the black symbols in Fig. 4A and B, in which the Reynolds number is exactly the same. Such an effect was also reported by Pereira and Soares (2012). The authors argue that an increasing concentration causes a more intense flow disturbance at the beginning of the process and consequently the time to reach a steady state turbulent structure is also increased. In PAM and XG solutions the effect of concentration on t_d was not very noticeable. The developing time seems to be very related to the polymeric flexibility. In other words, t_d seems to be very short for solutions of rigid molecule. Fig. 4B, D and F are displayed to provide a direct comparison between each polymer. The tests were carried out for the same range of Reynolds number and the same concentration and temperature. Considering PEO and PAM, (B) and (D), we can see that DR_{max} is slightly larger in PEO solutions, but DR_{asy} is considerably more pronounced in PAM solutions. This is evidently related to the fact that the degradation is more intense in PEO solutions. Even though higher levels of DR are achieved with use of PEO, the mechanical molecular scissions act more intensely in such a polymer and its final level of drag reduction is greatly reduced. It can also be concluded that the highest level of drag reduction is achieved more quickly in PAM solutions with increasing Reynolds numbers. This fact can be perceived by analysing the change of the Reynolds number from its smallest value ($Re = 733$) to the intermediate one ($Re = 1047$). The blue and black curves are closer to each other for PAM. A direct comparison between XG and the other molecules are not evident because the results for this polymer were obtained with a smaller molecular weight. However some comparisons can be highlighted. The first one is concerned with the loss of efficiency, which is more pronounced in PEO solutions, which have higher molecular weight. The second conclusion is related to the Reynolds number effect. As with PAM, the increase in DR with increasing Re is less significant with XG than with PEO. The results displayed in (E) and (F) confirm that the Reynolds number is, in fact, much less effective in XG solutions, as reported by Bewersdorff and Singh (1988) and Bewersdorff and Berman (1988). It seems that $Re = 733$ is very close to the onset and an increase in this parameter moves DR to a value very close to its maximum, for the specific concentration. This is consistent with the idea that XG's structure at rest is already extended and can work even at a low level of turbulence, the Type B mechanism of drag reduction reported by Virk *et al.* (1997).

Figure 4. Effect of Reynolds number on DR as a function of time.

Fixing again the temperature ($T=25^{\circ}\text{C}$) and Reynolds number ($Re = 1360$), Fig. 5 shows the effect of the concentration on $DR(t)$ for our three drag reducers (PEO, PAM and XG). As expected and widely reported by a number of researchers, DR increases with an increasing concentration. This is evident in all drag reducers used here. Concerning PEO and PAM, (A) and (B), the concentration of 100 ppm seems to be close to the MDR asymptote. Thus, the DR_{max} for both materials is very close to each other (approximately 0.23). For any other value of the concentration, the ultimate level of drag reduction is higher in PEO solutions. It is worth noting that a very small amount of PEO (2 ppm) causes a significant reduction in the drag (maximum value of 0.14). The same quantity of PAM provides the maximum drag reduction of 0.07, just one-half of the previous one. When the concentration of both polymers is continuously increased, we observe clearly that the growth of DR is more pronounced in PAM solutions. In other words, the curves of different concentrations of PEO are closer to each other. With respect to the XG solutions, Fig. 5(C), the changes in DR with concentration are gradual, as in PAM solutions. However, as the molecular weight in this case is smaller, this is not a conclusive comparison. An interesting point that deserves our attention is the fact that, with 100 ppm of XG, the DR_{max} achieves a value around 0.27. For PEO and PAM, the maximum value of DR achieved is 0.23, which is, supposedly, close to the MDR. Thus, possibly, the XG solution of 100 ppm is providing a drag reduction beyond the MDR asymptote.

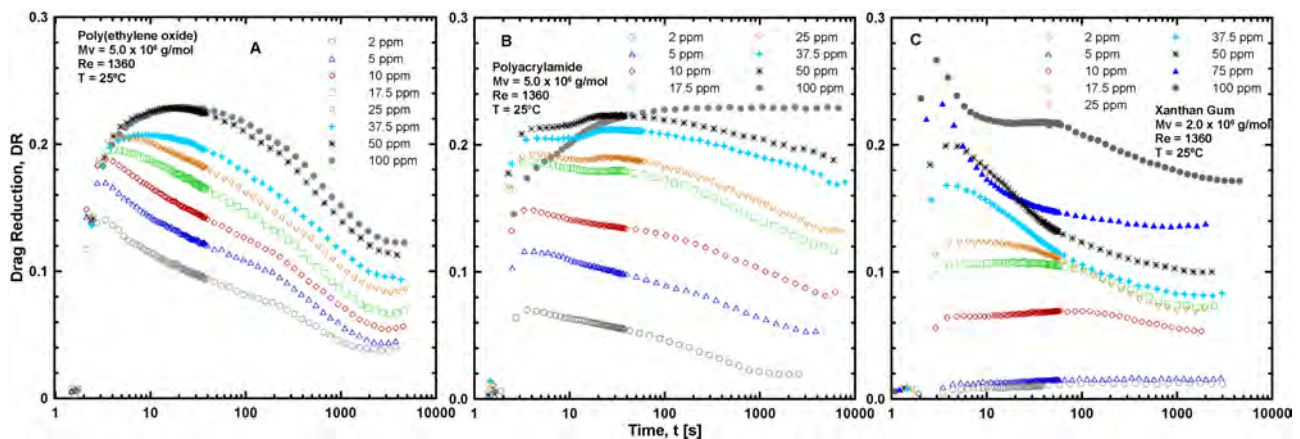


Figure 5. Effect of concentration on DR as a function of time.

It is interesting to note that t_d seems to have a rather weak relation to the concentration of XG and PAM, whereas the relation between t_d and c is very strong in PEO solutions, as reported by Pereira and Soares (2012). For PAM and XG solutions, DR_{max} is achieved in less than 3 seconds, even for the highest concentration of each polymer. This is probably related to molecule rigidity and it is worthy of attention. As reported numerically by Dimitropoulos *et al.* (2005), the turbulent structures take time to rearrange and achieve their final form after a large polymer deformation. In fact, we suppose that the steady state flow is achieved when the necessary number of molecules is working in a state of equilibrium with the turbulent structures. Definitely, this state of equilibrium is sensitive to the molecular scission and to any change in the molecular structural configuration and the developing time increases when degradation or changes in the molecular configuration plays a important role in the process. Hence, smaller values of t_d are to be expected for PAM and XG solutions as these two kinds of polymers are more mechanically resistant. Especially for the XG, its molecular configuration does not change significantly at the beginning of the test. Hence, this very fast developing time observed for XG is consistent with the idea of a Type B drag reduction mechanism.

A practical aspect of the problem that is worth attention is concerned with the resistance of the highly concentrated solution of PAM. In Fig. 5B we observe that the maximum level of efficiency is maintained over all the test time for the solution of 100 ppm. This observation contributes to the hypothesis that PAM solutions are stronger than PEO solutions (see Elbing *et al.* (2011)). Regarding the solution's resistance, the results for XG are quite curious. In contrast to the other polymers, XG solutions with very small concentrations ($c \leq 5$ ppm) showed no loss of efficiency, suggesting that molecular degradation does not play an important role in these solutions. In fact, what is more curious is that the loss of efficiency appears when the concentration is increased. Clearly, the period of time in which the maximum level of DR is maintained falls with increasing concentration. Such a fall is abrupt at very high values of concentration, $c \geq 75$ ppm. It is also worth noting that the curve of $c = 100$ ppm is quite different from all the other results. After the abrupt DR decrease at the very beginning of the test, the drag reduction achieves a constant level before it starts to decrease again. Such observations concerned with the effect of concentration in XG solutions are considerably distinct from those noticed in the other polymers, PEO and PAM. The particular way in which the XG decay curve appears is worth attention. There are clearly two power-law regions between DR_{max} and DR_{asy} , whereas in PEO and PAM only one power-law region is seen. We will return to this point again.

The effect of temperature on drag reduction, DR , as a function of time, t , is displayed in Fig. 6. The measurements were carried out for PEO, PAM and XG at a fixed Reynolds number ($Re = 1360$) in two different concentrations. For

each polymer, the temperature seems to play a more important role for the less concentrated solution. In other words, an increase in the temperature causes an increase in DR more pronounced at smaller concentrations. Such evidence can be observed when comparing the black and blue curves in Fig. 6C and D. When T is changed from 25°C to 35°C , the growth of DR in the PAM solution of 10 ppm is significantly larger. The same conclusion can also be seen by observing the black and red curves of the PEO solutions, (A) and (B). The evidence is not clear for XG. Observing the data for each material, Figures (B), (D) and (F), we have an impression that the drag reduction is more affected by temperature in XG solutions. Regarding the data in (E), we can conclude that DR is, in fact, highly influenced by temperature. From 20°C to 40°C , DR changes significantly its decay function. At 20°C , the green symbols, it is easy to perceive three power-law regimes in $DR(t)$ between its maximum and asymptotic level. The curve for 25°C , black symbols, is characterized by two power-law regimes, whereas in temperatures larger than 30°C only one power-law regime is perceived. Up from this level of temperature, the XG decay function is quite similar to that observed for PEO solutions. It is worth noting that DR is considerably increased in PAM and XG solutions. Increasing the temperature from 25°C to 45°C , the value of DR_{max} in PEO, PAM and XG solution was increased by, respectively, 20%, 26% and 35%. As to the XG solutions, increasing the temperature below the *transition-midpoint temperature* provides an increase in the mean length of the molecule, which probably causes an increase in DR .

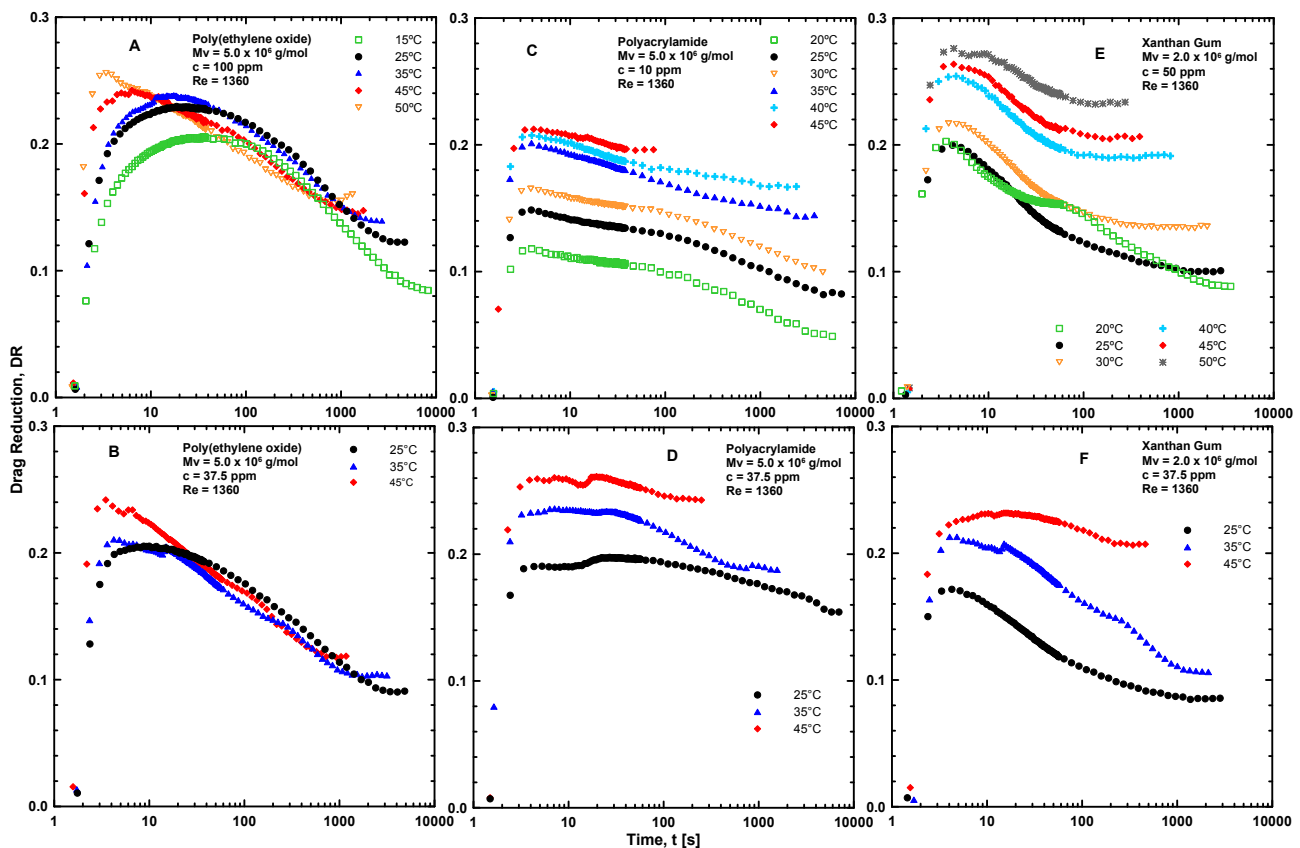


Figure 6. Effect of temperature on drag reduction, DR , as a function of time, t .

3.3 The relative drag reduction decay

In this subsection we display the relative drag reduction against the time from the maximum level of efficiency to its asymptotic value after a long enough time. Hence, DR' varies between 0 and 1. This style of data exhibition is an attempt to look directly at the loss of efficiency related to the mechanical molecular scission.

Using data from Fig. 4, Fig. 7 shows DR' against time to clarify the effect of the Reynolds number on the loss of efficiency, $L_{ef} = 1 - DR'_{asy}$. A fall of L_{ef} is expected with increasing concentration. This is clearly observed in the PEO and PAM solutions, but not in the XG solutions. The black and blue curves of the more concentrated solution of PEO and PAM, respectively, (A) and (D), are closer to 1. In contrast, observing (E) and (F), it seems that the two curves are very similar to each other. In fact, DR'_{asy} for the two concentrations of XG, at the same Reynolds number, are practically identical. We will return to this point later when the effect of the concentration of XG is reported. Comparing the different polymers, it is very clear that the PAM solutions present the smallest loss of efficiency. At the maximum Reynolds number

($Re = 1360$), L_{ef} is only 20% in PAM solutions, whereas it is 50% and 55% for XG and PEO solutions, respectively. As the maximum efficiency is expected for the smallest Reynolds number, DR' at $Re = 733$ behaves strangely, at least at first glance, in the PEO and XG solutions. We suppose this value of Re is very close to the onset of the drag reduction and, after a period of time, a great amount of degraded molecules, or tangled in the case of XG, stop being stretched and interact with the turbulent structures. In other words, the $Re = 733$ is below the onset Reynolds number for a significant number of degraded or tangled molecules. We suppose this is the cause of the abrupt fall of efficiency and the observed intersection of the curves.

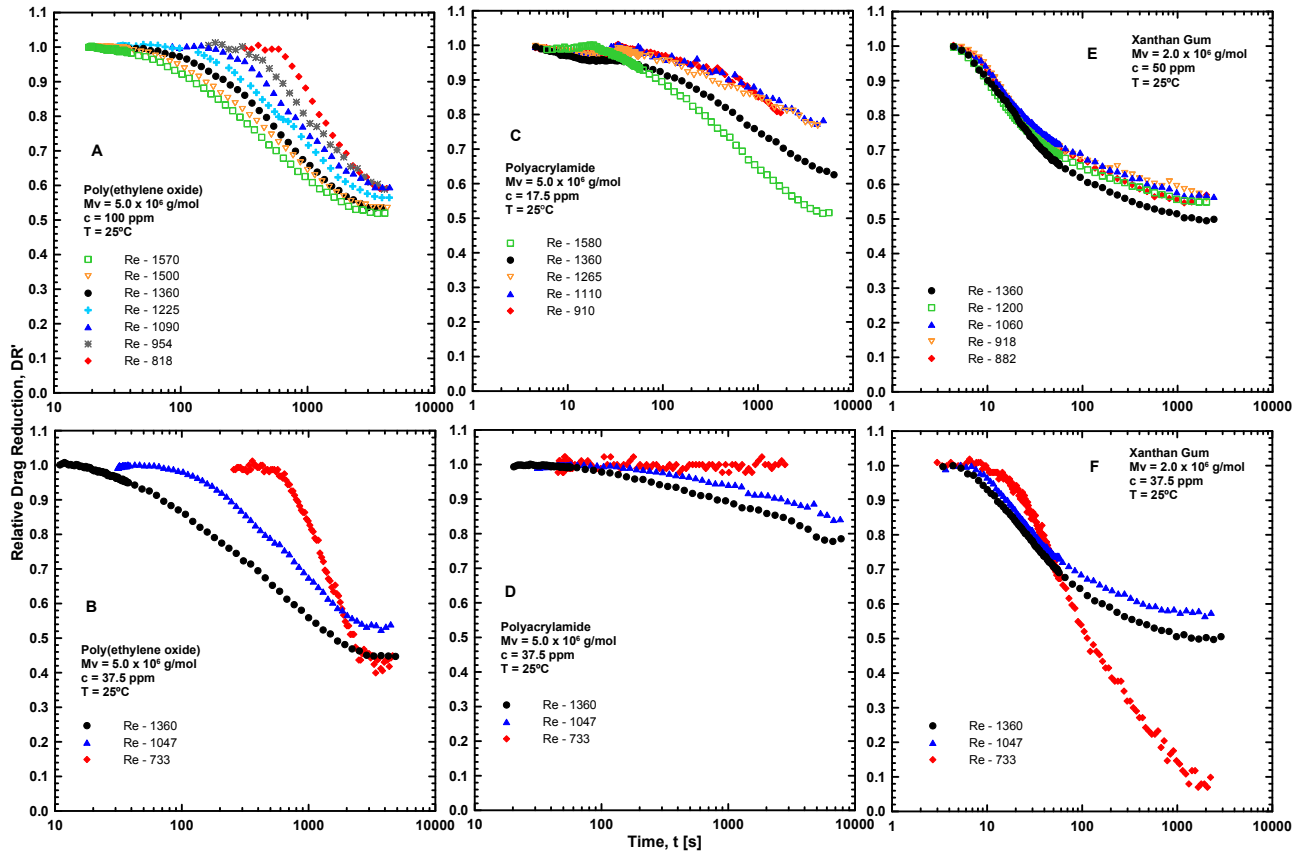


Figure 7. Effect of Reynolds number on DR' as a function of time.

Using data from Fig. 5, Fig. 8 displays $DR'(t)$. Figures A, B and C show that the efficiency of drag reduction is strongly dependent on the concentration c . For PEO and PAM solutions, L_{ef} is considerably reduced with increasing c . Supposedly, the loss of efficiency for flexible polymers is related to polymer degradation and the solution resistance increases with increasing concentration. Thus, such an effect on DR' is expected. It is interesting to note here that the PAM solution of $c = 100$ ppm does not lose efficiency. In other words, DR' is kept at its maximum level over all the test time, around 2 hours. Comparing (A) and (B), we can conclude that the efficiency of PAM solutions is notably larger than that of the PEO solutions. The data for the XG solutions, depicted in Fig. 8C, show an effect of concentration considerably different from the other polymers and quite curious, at first glance. For the range of concentration $2 \leq c \leq 37.5$ ppm, DR' falls with increasing c . After $c = 37.5$ ppm, the effect of concentration is similar to that observed for PEO and PAM, and DR' rises with an increase in this parameter. As mentioned before, we believe this effect is related to changes in the microstructure of XG with increasing concentration. At very small values of c , in this case $c \leq 5$ ppm, the XG microstructure is helicoidal, there is no change in its microstructure during the test, and L_{ef} is equal to 1. Increasing the concentration, the helical form becomes unstable under turbulence and some of the molecules change their conformation from the helical to the tangled form. We suppose the change of configuration is intensified by the turbulence and a loss of efficiency is perceived. Hence, possibly, a great part of the loss of efficiency observed could be related to changes in the microstructure of the Xanthan Gum.

Fig. 9 shows the effect of temperature on the relative drag reduction using the data from Fig. 6. The effect of temperature on the drag reduction efficiency is really complex. For PEO solutions, whose results are displayed in (A) and (B), we can observe that an increasing temperature accelerates the loss of efficiency, but the asymptotic value of DR' increases with temperature, at least for the range of temperature below 45°C . It seems that DR'_{asy} starts to fall for increments of T above this value. The dependence of DR' on temperature is quite similar in PAM solutions. DR'_{asy} also increases with an

Anselmo S. Pereira, Raphael M. Andrade, and Edson J. Soares

Drag Reduction Induced by Flexible and Rigid Molecules in a Turbulent Flow Into a Rotating Cylindrical Double Gap Device

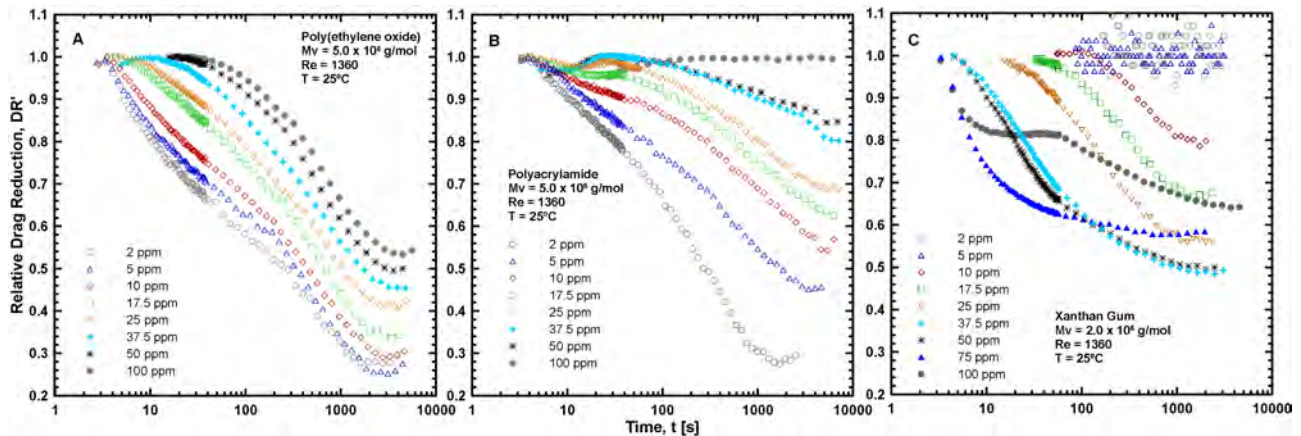


Figure 8. Effect of concentration on DR' as a function of time.

increasing temperature. The role of temperature at the smallest concentrated PAM solution, (C), is more pronounced than in the solution of 37.5 ppm, (D). Such a difference is not observed in the PEO solutions. Temperature also plays a very significant role in the XG solutions, especially in the less concentrated solution, where the difference in DR' between $25^\circ C$ and $45^\circ C$ is clearly more pronounced. The shape of $DR'(t)$ changes considerably from $20^\circ C$ to $25^\circ C$ in the more concentrated solution, (E). As in other polymers, DR'_{asy} increases with an increasing temperature.

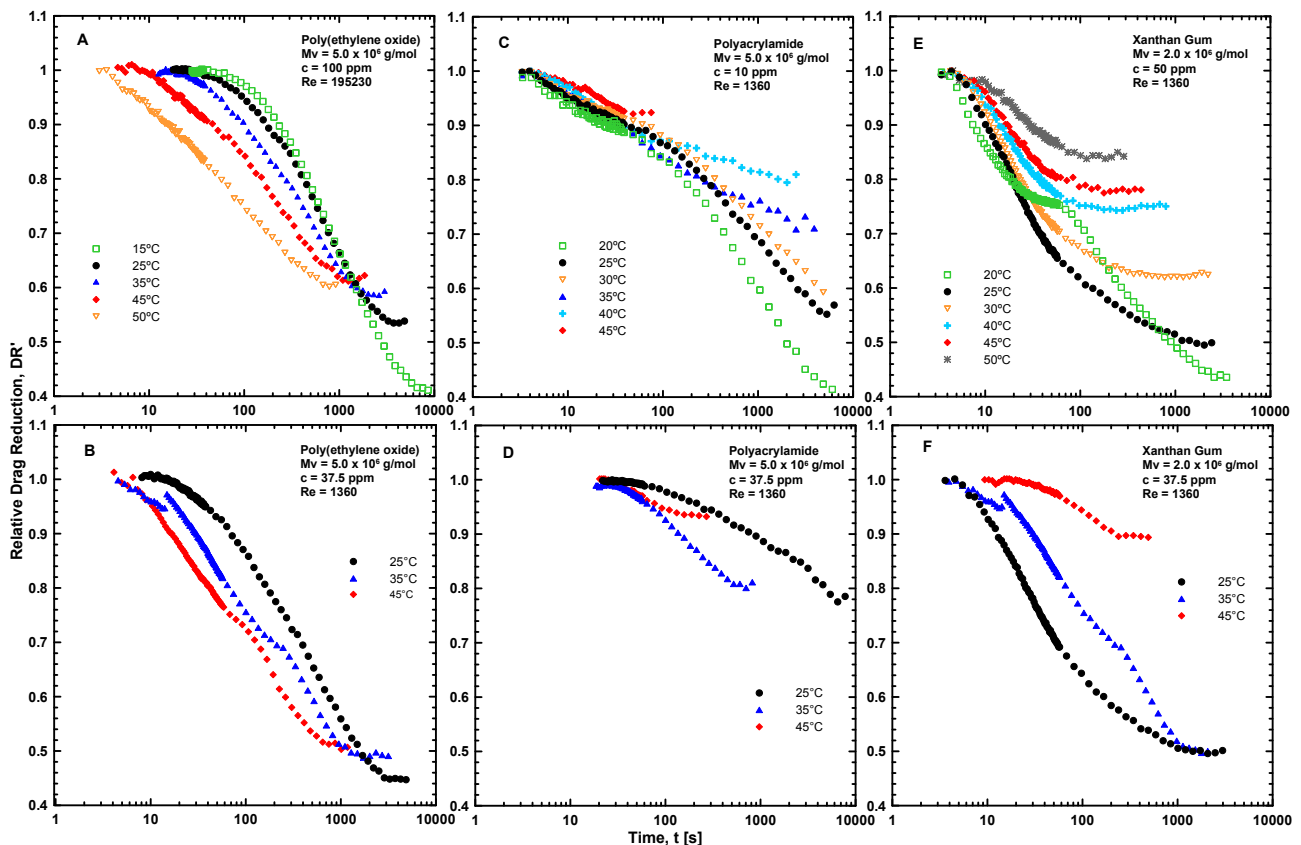


Figure 9. Effect of temperature on the relative drag reduction, DR' , as a function of time, t .

4. FINAL REMARKS

We have analyzed the evolution of the drag reduction over time for three polymers, PEO, PAM and XG. The first and second are flexible polymers and the third is a rigid polymer. A wide range of Reynolds numbers, concentrations, and temperatures were studied from the very beginning of the test until the asymptotic value of DR was achieved. The main results were displayed in an attempt to provide a direct comparison between all three polymers.

As reported by many researchers, our results show that the Reynolds number plays a weak role in DR and DR' for Xanthan Gum solutions. This is very different from what is observed for PEO and PAM, where Re is quite important. In fact, the mechanism of drag reduction in rigid polymers is very different from that in flexible ones and it is related to the molecules's microstructure, as reported by Virk *et al.* (1997). Concerning the concentration, it is worth noting that no loss of DR was observed for high values of c in the PAM solutions. This suggests that PAM is more resistant than PEO, though the last one provides higher values of DR_{max} . As expected, the level of drag reduction, DR , and its efficiency, DR' , increases with an increasing concentration for PEO and PAM. However, the relative drag reduction dependency on concentration for Xanthan Gum solutions showed a considerably different behavior. With an increasing concentration, DR' falls before starting to increase again. We believe such an effect is mostly related to a change in the microstructure of the XG from the helical form to the tangled configuration, which is helped by the flow.

Temperature plays a very important role in DR , specially in XG solutions. An increase in T below the *transition-midpoint temperature* causes a significant gain in the efficiency of Xanthan Gum. At 45°C, the loss of efficiency is only slightly perceived.

5. ACKNOWLEDGEMENTS

This research was partially funded by grants from the CNPq (Brazilian Research Council), the ANP (Brazilian Petroleum Agency), and Petrobras.

6. REFERENCES

- Benzi, R., 2010. "A short review on drag reduction by polymers in wall bounded turbulence". *Physical D*, Vol. 239, pp. 1338–1345.
- Berman, N.S., 1978. "Drag reduction by polymers". *Annual Reviews of Fluid Mechanics*, Vol. 10, pp. 47–64.
- Bewersdorff, H.W. and Berman, N.S., 1988. "The influence of flow-induced non-newtonian fluid properties on turbulent drag reduction". *Rheologica Acta*, Vol. 27, pp. 130–136.
- Bewersdorff, H.W. and Singh, R.P., 1988. "Rheological and drag reduction characteristics of xanthan gum solutions". *Rheologica Acta*, Vol. 27, pp. 617–627.
- Bizoto, V.C. and Sabadini, E., 2008. "Poly(ethylene oxide) x polyacrylamide". *Journal of Applied Polymer Science*, Vol. 25, pp. 1844–1850.
- Burger, E.D. and Chorn, L.G., 1980. "Studies of drag reduction conducted over a broad range of pipeline conditions when flowing prudhoe bay crude oil". *J. Rheology*, Vol. 24, p. 603.
- Choi, H.J. and Jhon, M.S., 1996. "Polymer-induced turbulent drag reduction". *Industrial and Engineering Chemistry Research*, Vol. 35, pp. 2993–2998.
- Choi, H.J., Kim, C.A., Sohn, J. and Jhon, M.S., 2001. "An exponential decay function for polymer degradation in turbulent drag reduction". *Carbohydrate Polymers*, Vol. 45, pp. 61–68.
- Deshmukh, S.R. and Singh, R.P., 1986. "Drag reduction characteristics of graft copolymers of xanthan gum and polyacrylamide". *Journal of Applied Polymer Science*, Vol. 32, pp. 6163–6176.
- Dimitropoulos, C.D., Dubief, Y., Shaqfeh, E.S.G., Moin, P. and Lele, S.K., 2005. "Direct numerical simulation of polymer-induced drag reduction in turbulent boundary layer flow". *Physics of Fluids*, Vol. 17, pp. 1–4.
- Dubief, Y., White, C.M., Terrapon, V.E., Shaqfeh, E.S.G., Moin, P. and Lele, S.K., 2004. "On the coherent drag-reducing and turbulence-enhancing behaviour of polymers in wall flows". *J. Fluid Mech*, Vol. 514, pp. 271–280.
- Elbing, B.R., Solomon, M.J., Perlin, M., Dowling, D.R. and Ceccio, S.L., 2011. "Flow-induced degradation of drag-reducing polymer solutions within a high-reynolds- number turbulent boundary layer". *J. Fluid Mech*, Vol. 670, pp. 337–364.
- Fabula, A.G., 1971. "Fire-fighting benefits of polymeric friction reduction". *Trans ASME J Basic Engng*, pp. 93–453.
- Flory, P.J., 1971. *Principles of Polymer Chemistry*. Cornell University Press, Ithaca, NY.
- Gasljevic, K., Aguilar, G. and Matthys, E.F., 2001. "On two distinct types of drag-reducing fluids, diameter scaling, and turbulent profiles". *Journal of Non-Newtonian Fluid Mechanics*, Vol. 96, pp. 405–425.
- Greene, H.L., Mostardi, R.F. and Nokes, R.F., 1980. "Effects of drag reducing polymers on initiation of atherosclerosis". *Polym Engng Sci*, pp. 20–449.
- Jaafar, A.J., Escudier, M.P. and Poole, R.J., 2009. "Turbulent pipe flow of a drag-reducing rigid rod-like polymer solution". *Journal of Non-Newtonian Fluid Mechanics*, Vol. 161, pp. 86–93.
- Kalashnikov, V.N., 1998. "Dynamical similarity and dimensionless relations for turbulent drag reduction by polymer additives". *Journal of Non-Newtonian Fluid Mechanics*, Vol. 75, pp. 209–230.
- Kalashnikov, V.N., 2002. "Degradation accompanying turbulent drag reduction by polymer additives". *Journal of Non-Newtonian Fluid Mechanics*, Vol. 103, pp. 105–121.
- Kenis, P.R., 1971. "Turbulent flow friction reduction effectiveness and hydrodynamic degradation of polysaccharides and synthetic polymers". *Journal of Applied Polymer Science*, Vol. 15, p. 607.

Anselmo S. Pereira, Raphael M. Andrade, and Edson J. Soares

Drag Reduction Induced by Flexible and Rigid Molecules in a Turbulent Flow Into a Rotating Cylindrical Double Gap Device

- Kim, C.A., Lee, K., Choi, H.J., Kim, C.B., Kim, K.Y. and Jhon, M.S., 1985. "The turbulent drag reduction by graft copolymers of guar gum and polyacrylamide". *Journal of Applied Polymer Science*, Vol. 31, pp. 4013–4018.
- Kim, C.A., Lee, K., Choi, H.J., Kim, C.B., Kim, K.Y. and Jhon, M.S., 1997. "Universal characteristics of drag reducing polyisobutylene in kerosene". *Journal of Macromolecular Science Pure and Applied Chemistry*, Vol. A34, pp. 705–711.
- Lumley, J.L., 1969. "Drag reduction by additives". *Annual Review of Fluid Mechanics*, Vol. 11, pp. 367–384.
- Morris, E.R., 1977. "Molecular origin of xanthan solution properties". *Extracellular Microbial Polysaccharides, ACS Symposium Series*, Vol. 45, pp. 81–89.
- Moussa, T. and Tiu, C., 1994. "Factors affecting polymer degradation in turbulent pipe flow". *Chemical Engineering Science*, Vol. 49, pp. 1681–1692.
- Muller, G., Anhourrache, M., Lecourtier, J. and Chauveteau, G., 1986. "Salt dependence of the conformation of a single-stranded xanthan". *International Journal of Biological Macromolecules*, Vol. 8, pp. 167–172.
- Nakano, A. and Minoura, Y., 1975. "Relationship between hydrodynamic volume and the scission of polymer chains by high-speed stirring in several solvents". *Macromolecules*, Vol. 8, pp. 677–680.
- Nakken, T., Tande, M. and Elgsaeter, A., 2001. "Measurements of polymer induced drag reduction and polymer scission in Taylor flow using standard double-gap sample holders with axial symmetry". *Journal of Non-Newtonian Fluid Mechanics*, Vol. 97, pp. 1–12.
- Norton, I.T., Goodall, D.M., Frangou, S.A., Morris, E.R. and Ress, D.A., 1984. "Mechanism and dynamics of conformational ordering in xanthan polysaccharide". *Journal of Molecular Biology*, Vol. 175, pp. 371–394.
- Paterson, R.W. and Abernathy, F., 1970. "Turbulent flow drag reduction and degradation with dilute polymer solutions". *J. Fluid Mech*, Vol. 43, pp. 689–710.
- Pereira, A.S. and Soares, E.J., 2012. "Polymer degradation of dilute solutions in turbulent drag reducing flows in a cylindrical double gap rheometer device". *Journal of Non-Newtonian Fluid Mechanics*, Vol. 179, pp. 9–22.
- Peysner, P. and Little, R.C., 1971. "The drag reduction of dilute polymer solutions as a function of solvent power, viscosity, and temperature". *Journal of applied polymer science*, Vol. 15, pp. 2623–2637.
- Rho, T., Park, J., Kim, C., Yoonb, H. and Suhb, H., 1996. "Degradation of polyacrylamide in dilute solution". *Polymer Degradation and Stability*, Vol. 52, pp. 287–293.
- S. Chakrabarti, B. Seidl, J.V. and Brunn, P.O., 1991b. "Correlations between porous medium flow data and turbulent flow results for aqueous hydroxypropylguar solutions (part 2)". *Rheologica Acta*, Vol. 30, pp. 124–130.
- Sellin, R.H.J., Hoyt, J.W., Poliart, J. and Scrivener, O., 1982. "The effect of drag reducing additives on fluid flows and their industrial applications part ii: present applications and future proposals". *Journal of Hydraulic Research*, Vol. 20, pp. 235–292.
- Sohn, J.I., Kim, C.A., Choi, H.J. and Jhon, M.S., 2001. "Drag-reduction effectiveness of xanthan gum in a rotating disk apparatus". *Polymer Degradation and Stability*, Vol. 69, pp. 341–346.
- Tabata, M., Hosokawa, Y., Watanabe, O. and Sohma, J., 1986. "Direct evidence for main chain scissions of polymers in solution caused by high speed stirring". *Polymer Journal*, Vol. 18, pp. 699–712.
- Tabor, M. and de Gennes, P.G., 1986. "A cascade theory of drag reduction". *Europhysics Letter*, Vol. 7, pp. 519–522.
- Vanapalli, S.A., Islam, T.M. and Solomon, J.M., 2005. "Scission-induced bounds on maximum polymer drag reduction in turbulent flow". *Physics of Fluids*, Vol. 17.
- Virk, P.S., 1975a. "Drag reduction by collapsed and extended polyelectrolytes". *Nature*, Vol. 253, pp. 109–110.
- Virk, P.S., 1975b. "Drag reduction fundamentals". *AIChE Journal*, Vol. 21, pp. 625–656.
- Virk, P.S., Mickley, H.S. and Smith, K.A., 1967. "The Toms phenomenon: turbulent pipe flow of dilute polymer solutions". *Journal of Fluid Mechanics*, Vol. 22, pp. 22–30.
- Virk, P.S., Mickley, H.S. and Smith, K.A., 1970. "The ultimate asymptote and mean flow structure in Toms' phenomenon". *ASME-Journal of Applied Mechanics*, Vol. 37, pp. 488–493.
- Virk, P.S., Sherman, D.C. and Wagger, D.L., 1997. "Additive equivalence during turbulent drag reduction". *AIChE Journal*, Vol. 43, pp. 3257–3259.
- White, C.M. and Mungal, M.G., 2008. "Mechanics and prediction of turbulent drag reduction with polymer additives". *Annual Review of Fluid Mechanics*, Vol. 40, pp. 235–256.
- Wyatt, N.B., Gunther, C.M. and Liberatore, M.W., 2011. "Drag reduction effectiveness of dilute and entangled xanthan in turbulent pipe flow". *Journal of Non-Newtonian Fluid Mechanics*, Vol. 166, pp. 25–31.
- Yu, J.F.S., Zakin, J.L. and Patterson, G.K., 1979. "Mechanical degradation of high molecular weight polymer in dilute solution". *Journal of Applied Polymer Science*, Vol. 23, pp. 2493–2512.

7. RESPONSIBILITY NOTICE

The authors are the only responsible for the printed material included in this paper.